Journal of Imaging Science and Technology® 53(1): 010505–010505-8, 2009.

Effect of Toner Charge on Developing Behavior in Two-Component Electrophotographic System by Discrete Element Method

H. Mio▲
Research Center for Advanced Science and Technology, Doshisha University, Kyoto 610-0321, Japan and Kyoto Fine Particle Technology, Keihanna Interaction Plaza, Inc., Kyoto 619-0237, Japan
E-mail: hirosmio@gmail.com

J. Kawamura, R. Higuchi, A. Shimosaka, Y. Shirakawa, and J. Hidaka
Department of Chemical Engineering and Materials Science, Doshisha University, Kyoto 610-0321, Japan

Abstract. *The objective of this paper is to investigate the effect of toner charge on the developed toner mass in a two-component development process using the discrete element method. The behavior of toner particles having homogeneous charge* (−40 to+140 μC/g) *or distributed charges (which were measured in experimental work) were simulated. When toner particles had extremely large charge, they failed to adhere properly on the latent images, because only a few toners bridge the electric potential difference between the photoreceptor and the latent image. On the other hand, the adhesion force between toner and carrier was much larger than the electrostatic force under the conditions of smaller toner charge. Then, the toner particles could not fly to the latent image from the surface of carrier particles under the applied electric field. The adhered toner mass becomes large when the average charge is around* 25−45 μC/g. *In particular, homogeneous toner charge is better for printing with high efficiency.* © *2009 Society for Imaging Science and Technology.*
[DOI: 10.2352/J.ImagingSci.Technol.(2009)53:1(010505)]

INTRODUCTION

An electrophotographic system is one of the commonest printing technologies, and widely used for printers and copy machines. This system consists of mostly six processes; i.e., charging, exposure, development, transfer, fusing, and cleaning. The images are visualized by the toner particles, and they are controlled mainly by the electric fields. Thus, the charge of toner particles and their behavior in the electric field are very important for high quality of printed images. However, it is difficult to discuss the effect of toner charge on the printing efficiency on the basis of experimental approaches due to several reasons. The main reason is the difficulty of the observation of toner motion in the electrophotographic system.

Electropohotographic engines are being downsized and all the while the core elements of the machines are becoming more complicated to enable full-color printing. The size of toner particles is also very fine, and it is hard to know the effect of the toner charge of every particle during development. Therefore, numerical simulation for analyzing particle behavior is very useful in order to address these issues. The discrete element method (DEM)[1] is one of the best-known and reliable simulation methods for the analysis of solid particle behavior, and some research on the development process in the electrophotographic system employing this strategy has already been reported.[2–8]

However, it has been hard to simulate the large number of particles in DEM due to the calculation load. This is a serious problem in the case of the two-component developiment process, which uses two kinds of particles (toner and carrier particles) and has magnets in the development roll, as shown in Figure 1. The carrier (magnetic) particles form a magnetic brush on the development roll and carry toner particles to the development area. The ratio of particle sizes between them is around 7–10, and the toner concentration is about 8.0 wt %. Accordingly, a huge number of toner particles is required in the simulation of the two-component development process, and the calculation load of magnetic

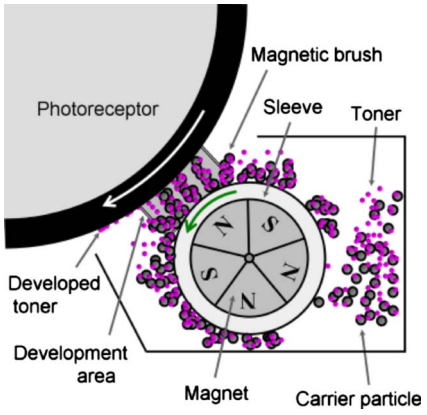

Figure 1. Two-component developing process.

▲IS&T Member

Received Jul. 12, 2008; accepted for publication Oct. 28, 2008; published online Feb. 4, 2009.
1062-3701/2009/53(1)/010505/8/$20.00.

force between carrier particles is also large. Therefore, a high-speed DEM algorithm is necessary for adequate studies on this process. The present authors have achieved acceleration of DEM by optimizing the particle detection process in the algorithm[9–11] and program tuning;[12] as well, a method for reducing the calculation load for estimating magnetic force between particles was also proposed.[13] This new DEM algorithm made the analysis of toner and carrier particles behavior in a two-component development process possible, and good agreement of the developed toner mass between the experimental work and the simulation was demonstrated.[14] The capability of this simulation technique has been reported in a previous paper.[14]

In this article, the development behavior in the two-component development process was simulated to find out the effect of toner charge on the developed toner mass using DEM. The toner charge was changed from -40 to $+140$ μC/g, and eight different toner charge distributions, which were measured in experimental work, were also used in the calculation, in order to simulate the actual process. The electric potential distribution was analyzed in more detail by considering the effects of the presence of magnetic brushes and toner particles around the development nip.

SIMULATION

Discrete Element Method

The three-dimensional particle behavior in the two-component development process was simulated using the DEM. DEM is one of the most popular and reliable simulation methods for the numerical analysis of solid particle behavior. This simulation method consists of the idea of determining the kinematic force to each finite-sized particle. All forces acting on each particle are modeled and calculated at every discrete-time step. The trajectories of particles are updated by Newton's law of motion, according to the following equations:

$$\dot{\mathbf{v}} = \frac{\Sigma \mathbf{F}}{m_g}, \tag{1}$$

$$\dot{\boldsymbol{\omega}} = \frac{\Sigma \mathbf{M}}{I}, \tag{2}$$

where $\mathbf{v}$ is the particle velocity, $\mathbf{F}$ is the summed force acting on a particle, m_g means the mass of a particle, $\boldsymbol{\omega}$ is the angular velocity, and $\mathbf{M}$ and I denote the moment of force and the moment of inertia. The contact force $\mathbf{F}_{CT}$, magnetic force $\mathbf{F}_M$, Coulomb force $\mathbf{F}_C$, electrostatic force $\mathbf{F}_E$, adhesion force $\mathbf{F}_v$, and gravitational force $\mathbf{F}_g$, act on carrier or toner particles in the two-component development process, and all forces are summed.

Contact Force

A contact model between two particles is given by the Voigt model, which consists of a spring dashpot and a slider for the friction in the tangential component. The contact forces $\mathbf{F}_n$, compressive, and $\mathbf{F}_t$, shear, can be calculated by the following equations:

$$\mathbf{F}_{n,ij} = \left(K_n \Delta u_{n,ij} + \eta_n \frac{\Delta u_{n,ij}}{\Delta t} \right) \mathbf{n}_{ij}, \tag{3}$$

$$\mathbf{F}_{t,ij} = \min \left\{ \mu_f |\mathbf{F}_{n,ij}| \mathbf{t}_{ij}, \left[K_t (\Delta u_{t,ij} + \Delta \varphi_{ij}) + \eta_t \left(\frac{\Delta u_{t,ij} + \Delta \varphi_{ij}}{\Delta t} \right) \right] \mathbf{t}_{ij} \right\}, \tag{4}$$

where K and η designate the spring and the damping coefficients, as given by Eqs. (5)–(8); Δu and $\Delta \varphi$ are the relative translational displacement of the gravitational center between two particles and the relative displacement at the contact point caused by the particle rotation, respectively. The frictional coefficient μ_f is particle-particle, 0.1; particle-photoreceptor, 0.58; and particle-sleeve, 0.5. The vectors $\mathbf{n}_{ij}$ and $\mathbf{t}_{ij}$ are the unit vectors from the ith particle to the jth one in normal and tangential components; the subscripts n and t also denote the normal and tangential components.

$$K_n = \frac{2}{3} \frac{E}{1 - \nu^2} b, \tag{5}$$

$$K_t = 8b \frac{1}{2(1+\nu)} \frac{E}{2(2-\nu)}, \tag{6}$$

$$\eta_n = 2\sqrt{m K_n}, \tag{7}$$

$$\eta_t = \eta_n \sqrt{\frac{K_t}{K_n}}, \tag{8}$$

where E and ν are Young's modulus (=0.1 GPa) and Poisson's ratio (=0.3), and b denotes the radius of the contact area.

Magnetic Force

Carrier particles in the magnetic field form magnetic brushes on the sleeve. The magnetic force is calculated from Eqs. (9)–(11).[15]

$$\mathbf{F}_{M,i} = (\mathbf{m}_i \cdot \nabla) \mathbf{B}_i, \tag{9}$$

$$\mathbf{B}_i = \mathbf{B}_{i,\text{field}} + \sum_{j=1(\neq i)}^{n} \mathbf{B}_{i,j}, \tag{10}$$

$$\mathbf{B}_{i,j} = \frac{\mu_0}{4\pi} \left[\frac{3(\mathbf{m}_j \cdot \mathbf{R}_{ji})}{|\mathbf{R}_{ji}|^5} \mathbf{R}_{ji} - \frac{\mathbf{m}_j}{|\mathbf{R}_{ji}|^3} \right], \tag{11}$$

where $\mathbf{m}_i$ and $\mathbf{B}_{i,\text{field}}$ mean the magnetic dipole moment of the ith particle and the magnetic flux density caused by the magnet roll at the position of the ith particle, respectively. $\mathbf{B}_{i,j}$ is the magnetic flux density caused by the magnetized jth particle; μ_0 is the magnetic permeability of vacuum

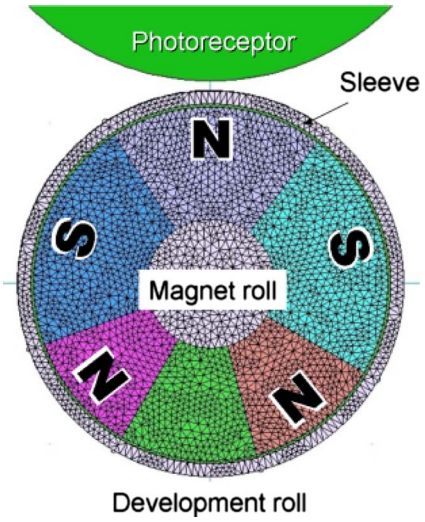

Figure 2. Magnet configuration.

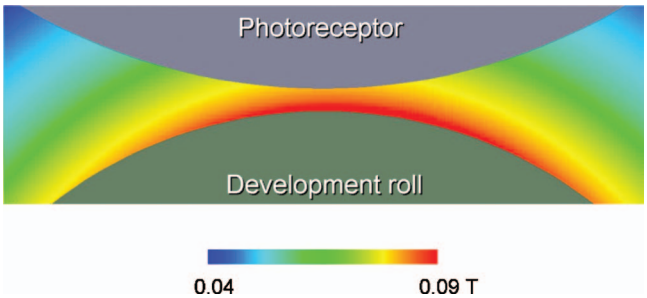

Figure 3. Distribution of magnetic flux density.

($=1.26\times10^{-6}$ H/m), and $\mathbf{R}_{ji}$ is the position vector from the jth particle to the ith one. The magnetic dipole moment is defined by Eq. (12).

$$\mathbf{m}_i = \frac{4\pi}{\mu_0}\frac{\mu_r - 1}{\mu_r + 2} r_i^3 \mathbf{B}_i, \tag{12}$$

where μ_r means the relative magnetic permeability, which was taken as 10,000 in this calculation. The magnetic flux density around the development roll was analyzed using J-MAG STUDIO version 8.3 (JRI Solutions, Ltd.). Figures 2 and 3 show the magnet configuration and the calculated results of magnetic flux density around the development nip, respectively.

Coulomb Force

Coulomb force $\mathbf{F}_C$, acts on toner/toner or toner/carrier particles, because the toner carries a triboelectric charge, which is established by agitation in a developer tank. $\mathbf{F}_C$ is calculated from the following equation:

$$\mathbf{F}_{C,ij} = \frac{1}{4\pi\varepsilon}\frac{q_i q_j}{|\mathbf{R}_{ji}|^2}\frac{\mathbf{R}_{ji}}{|\mathbf{R}_{ji}|}, \tag{13}$$

where ε is the permittivity of air ($=8.86\times10^{-12}$ F/m), and q denotes the charge on the toner. It was assumed that the toner particles have their charges at the center of the particles, not on the surface, because taking into consideration a distribution of charge on the toner surface is very difficult given the present level of computing power. The carrier particle has the opposite charge to the toner, and the charge on the carrier particle was also assumed to be removed quickly when the toner went away.

Table I. Adhesion force.

Toner/photoreceptor	[nN]	51.3
Toner/toner	[nN]	19.9
Toner/carrier	[nN]	32.5
Carrier/carrier	[nN]	88.2

Electrostatic Force

The toner particles, which are transported to the development nip area, fly to the latent images on the photoreceptor from the surface of magnetic brushes under the influence of the electrostatic force $\mathbf{F}_E$. A toner having charge q is subjected to $\mathbf{F}_E$ from the electric field $\mathbf{E}$.

$$\mathbf{F}_E = q\mathbf{E}, \tag{14}$$

$$\mathbf{E} = -\nabla\phi, \tag{15}$$

where ϕ is the electric potential, which is given by Eq. (16).

$$\nabla\cdot(-\varepsilon\nabla\phi) = \rho, \tag{16}$$

in which ρ denotes the charge density of the nip area, and ε is the permittivity. The electric potential distribution in the nip is affected by the presence of the magnetic brushes and charged toner particles.

Adhesion Force

The adhesion force between uncharged polymerized toner particles (diameter, $d_p=7.5$ μm) or uncharged toner and carrier ($d_p=41.8$ μm) particles was measured by the direct separation method[16] (PAF-300N, Okada Seiko Co. Ltd., Japan). A particle was stuck to another particle and it was subsequently pulled off. Table I shows the measured adhesion forces, and these forces were considered at the particle contact.

Simulation Conditions

Carrier particles (2605) of 40.0 or 50.0 μm diameter were mixed and positioned on the sleeve, and the magnetic brushes were formed initially by calculating only carrier particles. The monosized toner particles were adhered onto the magnetic brushes randomly, and Figure 4 shows the initial particle condition. The diameter of the toner particles was 8.0 μm, and the number of toner particles was 119,919. The densities of carrier or toner particles were 3600 or 1100 kg/m^3, and the toner concentration was 7.2 wt %. The conditions of homogeneous or distributed toner charge were calculated; i.e., the toner charge was changed from -40 to $+140$ μC/g in the case of homogeneous, and the eight different measured charge distributions of actual toner par-

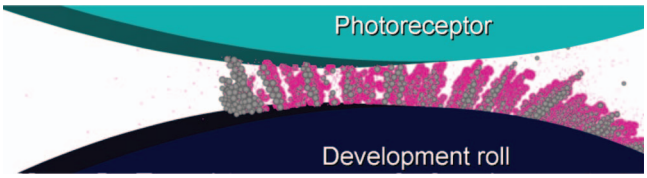

Figure 4. Initial particle condition.

ticles, which are shown in Figure 5, were used in the calculation. The toner charge distributions had been measured using E-Spart Analyzer (Model EST-II, Hosokawa Micron Corporation). It was assumed that the toner charge was at the center of the particle and that it did not change under motion. The diameters of the development roll or photoreceptor were 12 or 16 mm, respectively, and the development gap distance was 0.3 mm; their circumferential velocities were 0.61 or 0.59 m/s, and their direction at the development nip was forward. The axial length of the calculation area was shortened to 0.5 mm due to the calculation load, and the periodical boundary was also considered at the axial direction. The offset bias voltage and the peak-to-peak voltage were 300 and 1200 V, respectively. The frequency of the development field was 4.0 kHz, and its wave form was rectangular. The electric potential of the photoreceptor was 600 V, and the dot latent images were located on it. The electric potential distribution was calculated using the difference method. In order to consider the effect of the presence of a magnetic brush on the development field of carrier particles, relative permittivity of 5.0 was assumed for them. The toner charge around the nip was also considered in the electric potential calculation. The discrete time Δt for calculating particle behavior was 1.0×10^{-8} s, and the calculation was run for 0.73 million steps.

RESULTS AND DISCUSSION

Figure 6 shows the equipotential lines around the latent images. It was found that the electric potential distributions fluctuated from the presence of the magnetic brushes. Figure 7 shows a snapshot of development behavior under the condition of 25 μC/g of homogeneous toner charge. A movie is available over the Web (http://powder.doshisha.ac.jp/~mio/twocomp/development.avi). We observed that the dot images were being developed under these conditions. Figure 8 shows snapshots of developed toner particles on the photoreceptor under conditions of different homogeneous toner charges. The squares drawn in the figures identify the areas of latent image. The toners having 25 or 40 μC/g in charge adhered with better image quality than did those of other charge levels. On the other hand, the toner particles having extremely large or small charge could not adhere onto the latent images properly. When the toner charge is too large, only a few toners cover the electric potential difference between the photoreceptor and the latent image, as shown in Figure 9. Thus the image density decreases with increasing toner charge. Moreover, behavior of the toner particle could not be controlled by the development field when the toners

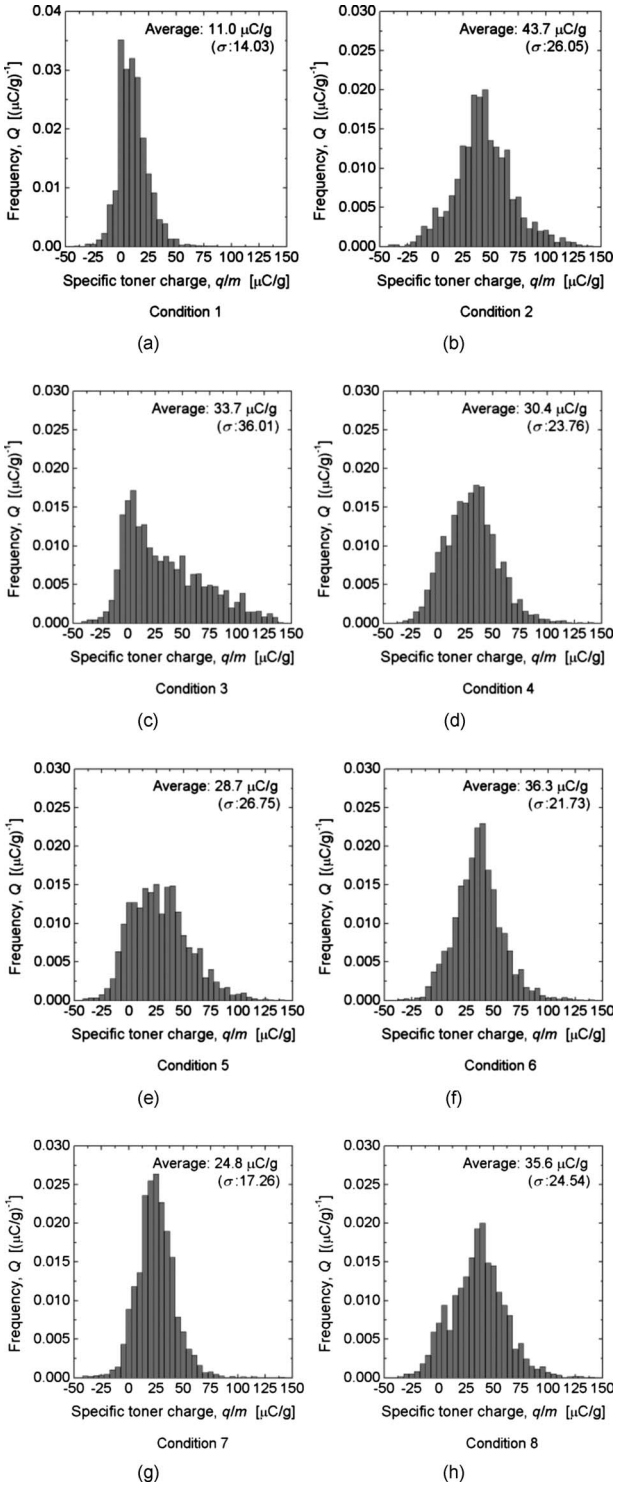

Figure 5. Toner charge distributions measured by E-Spart analyzer.

have the opposite charge, and most of the toner particles adhered outside of the latent images. This phenomena leads to the fog on the printed images.

Figure 10 shows the relationship between the adhered toner mass and the homogeneous toner charge. The toner particles having 25–40 μC/g seem to provide good development efficiency. The toner particles that are in the development nip are subjected mainly to three kinds of forces;

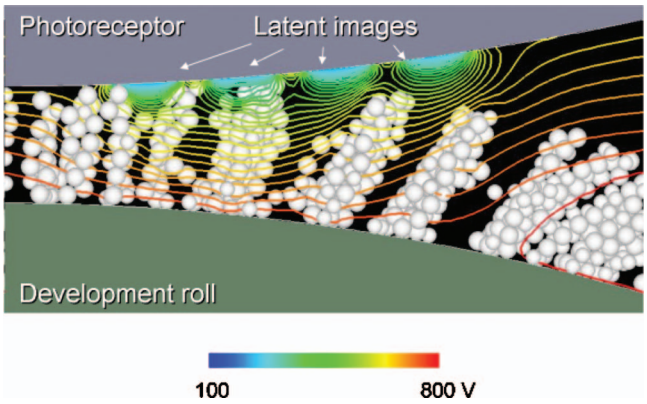

Figure 6. Equipotential lines around the latent images.

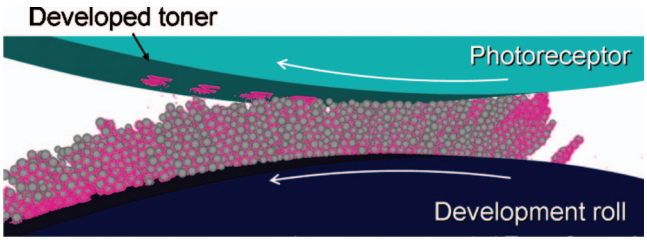

Figure 7. Snapshot of particle behavior during developing. The movie is available over the Web (http://powder.doshisha.ac.jp/~mio/twocomp/developing.avi).

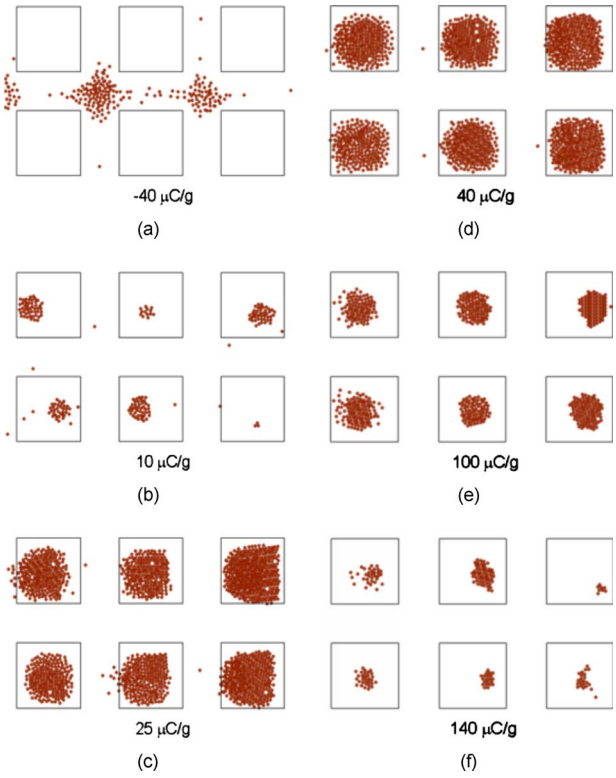

Figure 8. Snapshots of developed toner particles having different homogeneous charges.

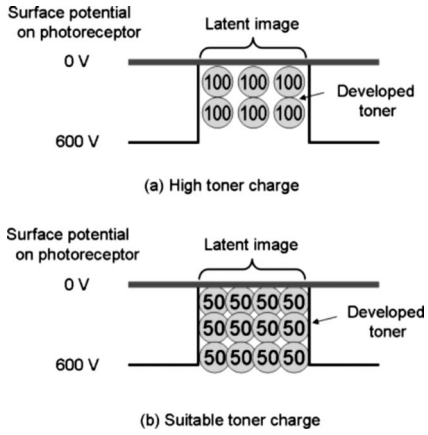

Figure 9. Schematic diagram of adhered toner particles on the photoreceptor.

i.e., the electrostatic force from the development field, Coulomb force, and adhesion force. These forces affect the development behavior strongly. Figures 11 and 12 show snapshots of development by toner particles with 10 or 40 μC/g charge. The colors of these toners designate the values of the forces. We found that the adhesion force between the toner and carrier is much larger than other forces when the toner has a 10 μC/g charge. Thus, the toner particles cannot fly to the latent image from the surface of carrier particles under the influence of the electrostatic force, because the adhesion force is dominant. This is the reason why the adhered toner mass decreases with decreasing toner charge. On the other hand, the forces acting on the toner particle seem to be well balanced for charge levels below 40 μC/g, and the toner behavior can be controlled by the development field. The electrostatic force around the edge of latent images is larger than that at the center, as shown in Fig. 12, which leads to the edge effect.

Figure 13 shows snapshots of developed toner particles having different charge distributions. The color of the particles designates the amount of charge. Although the toner particles having smaller charge seem to adhere near the edge of the image, most of the toners were well mixed. It is as though the particles having different charge are rearranging their positions during development. The particles having opposite or small charge did not adhere on the latent image, but some of them adhered on the outside. Thus these toners cause the fog phenomena on the printed image.

Figure 14 shows the effects of average toner change and the standard deviation σ of the charge distribution on the adhered toner mass. The size of each circle denotes the amount of adhered toner mass, and $\sigma=0$ means homogeneous toner charge. The adhered toner mass increases with a decreasing standard deviation of charge distribution, and it becomes large when the mean charge is around 25–45 μC/g. The toner particles cannot be developed for a smaller average charge, even if the standard deviation is small. This result correlates well with the result for homogeneous toner charge. Therefore, the toner should have 25–45 μC/g charge, and its charge distribution should be narrow. Although controlling the toner charge to obtain charge homogeneity is too difficult in practice, in principle

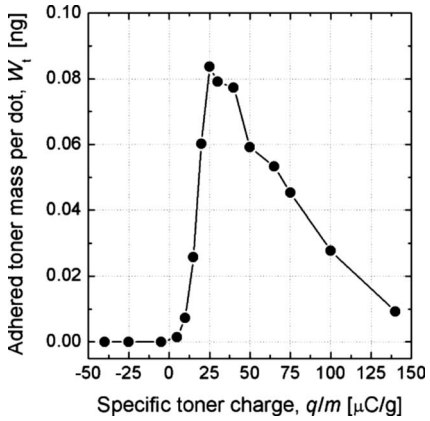

Figure 10. Relation between the adhered toner mass and the specific toner charge.

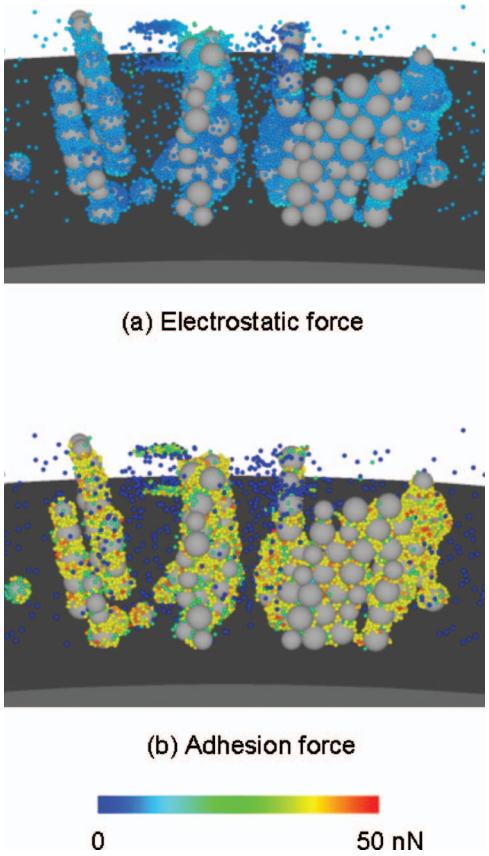

Figure 11. Snapshots of toner particles with different colors according to the force under 10 μC/g.

the homogeneous distribution is better for printing with high efficiency according to this analysis.

CONCLUSIONS

In this paper, the development behavior in the two-component development process was simulated by DEM to find out the effect of toner charge on the developed toner mass. Following is the summary of this work.

(i) The toner particles having extremely large charge could not adhere on the latent images properly, because only a few toners cover the electric potential difference between the photoreceptor and the latent image.

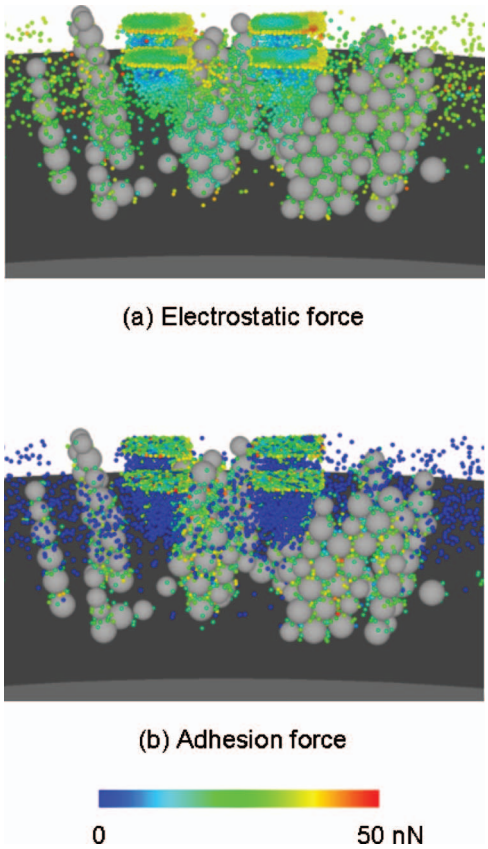

Figure 12. Snapshots of toner particles with different colors according to the force under 40 μC/g.

(ii) The adhesion force between the toner and carrier is much larger than the electrostatic force when the toner has a small charge. Thus, the toner particles cannot fly to a latent image from the surface of the carrier particles in the development field.

(iii) The behavior of toner could not be controlled by the development field under the condition of opposite toner charge, so most of the toner particles adhered onto the photoreceptor outside of the latent images.

(iv) The development behavior is controlled by the balance among the electrostatic force, Coulomb force, and adhesion force. The effect of adhesion force may seem to be large, because in this simulation the toner charge was assumed to be at the center of the toner particle.

(v) The adhered toner mass increases with decreasing standard deviation of charge distribution; it becomes large when the average charge is around 25–45 μC/g. The homogeneous toner charge is better for printing with high efficiency.

(vi) There were some assumptions in the simulation, i.e.,

- The toner charge is at the center of the particle.
- The charge does not change during motion.
- All particles have the same adhesion force, as measured in experimental work.

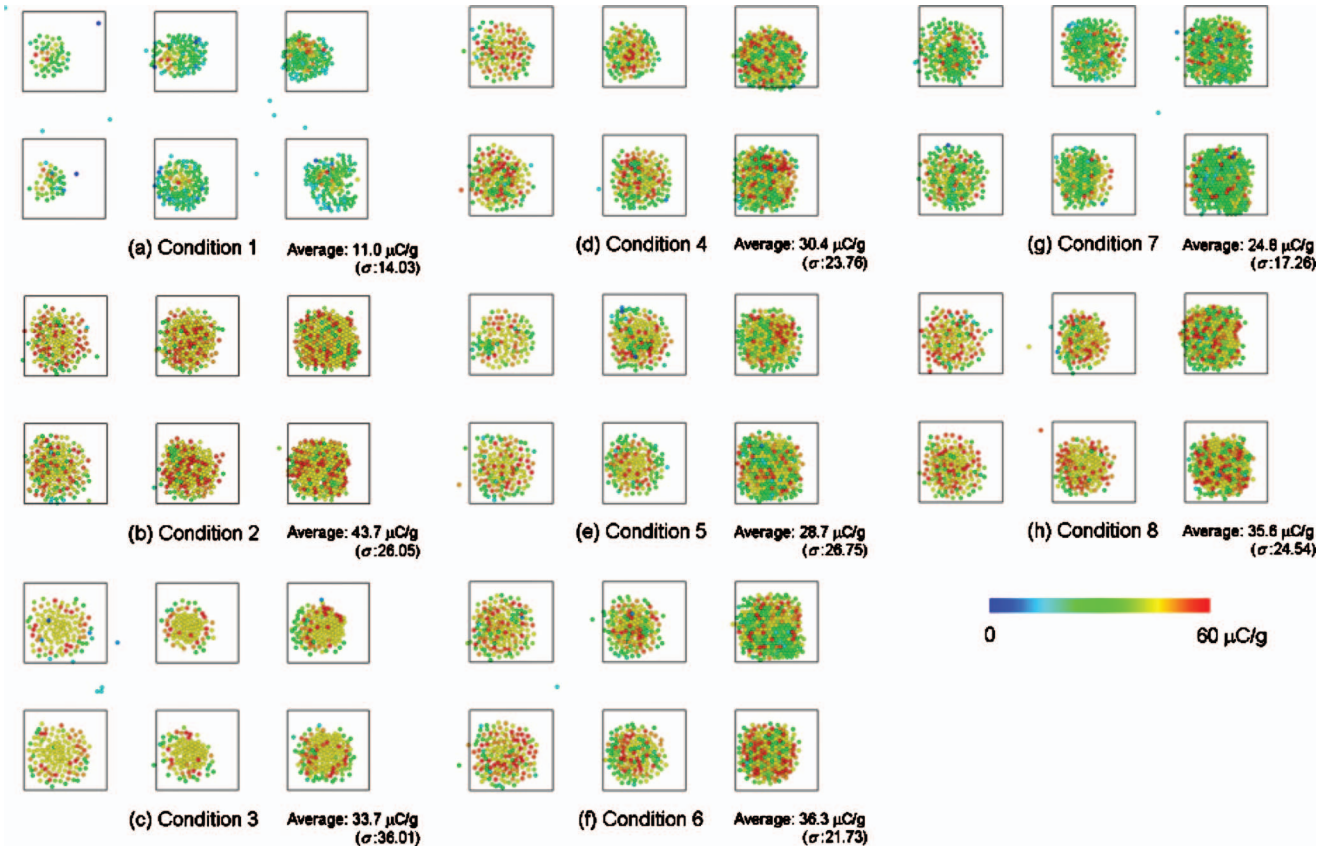

Figure 13. Snapshots of developed toner particles having different charge distributions.

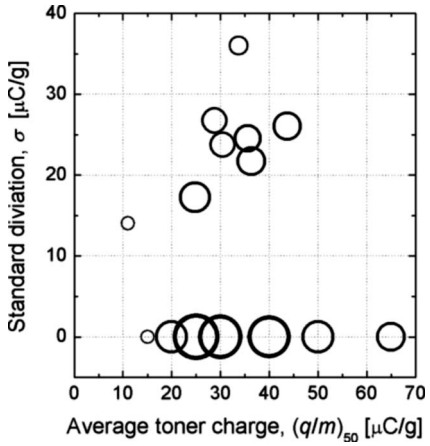

Figure 14. Effects of average toner change and the standard deviation of the charge distribution on the adhered toner mass.

- The toner particles do not have distributed size.
- All particles are spherical.

The grossest assumption seems that the toner charge is at the center of the particle. Therefore, the charge distribution on the toner surface is the next target to improve the simulation accuracy.

ACKNOWLEDGMENTS

The authors are grateful to JST (Japan Science and Technology Agency) for financial support to this project, along with the Kyoto Prefecture Collaboration of Regional Entities for the Advancement of Technological Excellence, and we wish to thank K. Tanida (Kyocera Mita Corporation) for kindly helping in the measurement of toner charge distribution.

REFERENCES

[1] P. A. Cundall and O. D. L. Strack, "A discrete numerical model for granular assemblies," Geotechnique **29**, 47–65 (1979).
[2] H. Kawamoto, "Transport of carriers in magnetic brush development process of electrophotography," J. Imaging Sci. Technol. **40**, 168–170 (1996).
[3] S. Serizawa, "Numerical simulation of development particle transport in electrophotography by distinct element method," Nihon Kikaigakkai Ronbunshu C. **64**, 3571–3576 (1998).
[4] J. Hidaka, Y. Sasaki, A. Shimosaka, and Y. Shirakawa, "Simulation of flow behavior of tow-component developer in electrophotographic system," Adv. Powder Technol. **13**, 317–332 (2002).
[5] N. Kuribayashi, T. Mitsuya, and N. Hoshi, "A numerical simulation for carrier particle behavior in electrophotographic magnetic brush development," Nihon Kikaigakkai Ronbunshu C. **68**, 71–78 (2002).
[6] N. Nakayama, H. Kawamoto, and S. Yamada, "Resonance frequency and stiffness of magnetic bead chain in magnetic field," J. Imaging Sci. Technol. **47**, 408–417 (2003).
[7] N. Nakayama, Y. Watanabe, Y. Watanabe, and H. Kawamoto, "Experimental and numerical study on the bead-carry-out in two component development process in electrophotography," J. Imaging Sci. Technol. **49**, 539–544 (2005).
[8] I. E. M. Severens, A. A. F. van de Ven, D. E. Wolf, and R. M. M. Mattheji, "Discrete element method simulations of toner behavior in the development nip of the Océ direct imaging print process," Granular Matter **8**, 137–150 (2006).
[9] H. Mio, A. Shimosaka, Y. Shirakawa, and J. Hidaka, "Optimum cell size for contact detection in the algorithm of discrete element method," J. Chem. Eng. Jpn. **38**, 969–975 (2005).

[10] H. Mio, A. Shimosaka, Y. Shirakawa, and J. Hidaka, "Optimum cell condition for contact detection having large particle size ratio in discrete element method," J. Chem. Eng. Jpn. **39**, 409–416 (2006).
[11] H. Mio, A. Shimosaka, Y. Shirakawa, and J. Hidaka, "Cell optimization for fast contact detection in the algorithm of discrete element method," Adv. Powder Technol. **18**, 441–453 (2007).
[12] H. Mio, A. Shimosaka, Y. Shirakawa, and J. Hidaka, "Program optimization for large-scale DEM and its effects of processor and compiler on the calculation speed," J. Soc. Powder Technol. Jpn. **44**, 206–211 (2007).
[13] H. Mio, Y. Matsuoka, A. Shimosaka, Y. Shirakawa, and J. Hidaka, "Speed-up Method for modeling of magnetic brush in two-component development system using discrete element method," J. Imaging Soc. Japan **46**, 95–102 (2007).
[14] H. Mio, Y. Matsuoka, A. Shimosaka, Y. Shirakawa, and J. Hidaka, "Analysis of development behavior in two-component development system by large-scale discrete element method," J. Chem. Eng. Jpn. **39**, 1137–1144 (2006).
[15] R. S. Paranjpe and H. G. Elrod, "Stability of chains of permeable spherical beads in an applied magnetic field," J. Appl. Phys. **60**, 418–422 (1986).
[16] Y. Shimada, Y. Yonezawa, and H. Sunada, "Measurement and evaluation of the adhesive force between particles by the direct separation method," J. Pharm. Sci. **92**, 560–568 (2003).